Modulating surface electron density of $Ni(OH)_2$ nanosheets with longitudinal $Ti_3C_2T_x$ MXene nanosheets by Schottky effect toward enhanced hydrogen evolution reaction

Xinyu Liu[a], Lan Wang[b*], Shan Ji[b], Vladimir Linkov[c], Qianqian Fu[a], Zhichao Li[a], Hui Wang [a*]

[a] College of Chemical Engineering, Qingdao University of Science and Technology, Qingdao, 266042, China

[b] Pinghu Normal College, Jiaxing University, Jiaxing 314001, China

[c] South African Institute for Advanced Materials Chemistry, University of the Western Cape, Cape Town, 7535, South Africa

Physical Characterization

X-ray diffraction (XRD) patterns were recorded on a Bruker D8 Advance instrument. Scanning electron microscopy (SEM) images were taken on a Carl Zeiss Ultra Plus. Transmission electron microscopy (TEM) images were taken on a JEOL JEM-2000FX and energy dispersive spectrometry (EDS) elemental mapping images were obtained using the same instrument. X-ray photoelectron spectroscopy (XPS) was conducted on a VG Escalab210 using Mg 300 W X as an X-ray source and the C 1 s peak at 285.0 eV as a reference binding energy calibration. Ultraviolet photoelectron spectroscopy (UPS) measurements were carried out on a Prevac spectrometer with a VG Scienta R3000 hemispherical electron energy analyzer. Photons with an energy of 21.22 eV generated by helium I were used for UPS spectrum generation. Specific surface areas of all prepared samples were obtained according to Brunauer-Emmett-Teller (BET) method.

Electrochemical performance tests

HER electrochemical tests were carried out in a three-electrode cell connected to the electrochemical workstation (CHI 660, CH Instruments) using as-prepared samples with a surface area of 1cm^2 as working electrodes and Hg/HgO, carbon rod and 1 M KOH as a reference electrode, counter electrode and electrolyte, respectively. The equation E_{RHE}= $E_{Hg/HgO}$ + 0.059 pH+ 0.14 V was used to establish the reversible hydrogen electrode (RHE) potential, and iR compensation was applied to all electrochemical experiments. Before tests, possible sample surface impurities were removed by scanning at -1~0.2 V with a scan rate of 50 mV s-1 followed by linear sweep voltammetry (LSV) in 1 M KOH electrolyte at a scan rate of 5 mV s-1. HER electrochemical impedance spectra (EIS) were obtained at potentials ranging from 0.1 Hz to 100 kHz. Tafel slopes of the samples were calculated using the Tafel equation η = blog j+ a, where b is the Tafel slope, η is the overpotential and j is the current density.

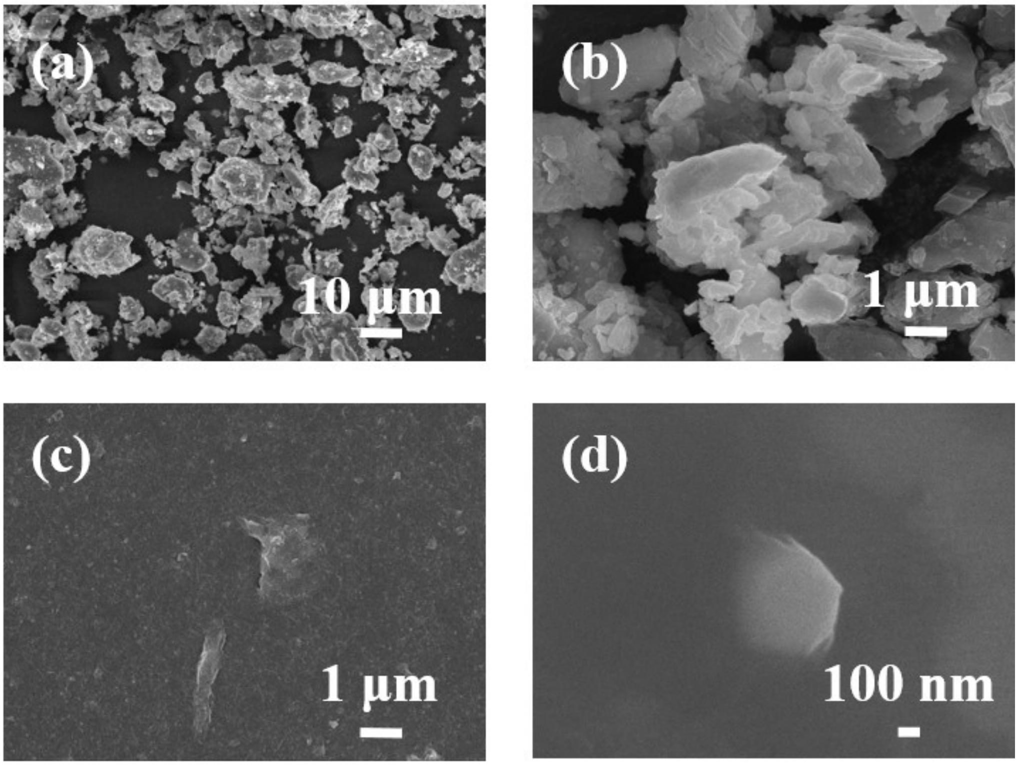

Figure S1. (a,b) SEM images of Ti_3AlC_2 MAX; (c,d) SEM images of $Ti_3C_2T_X$ MXene.

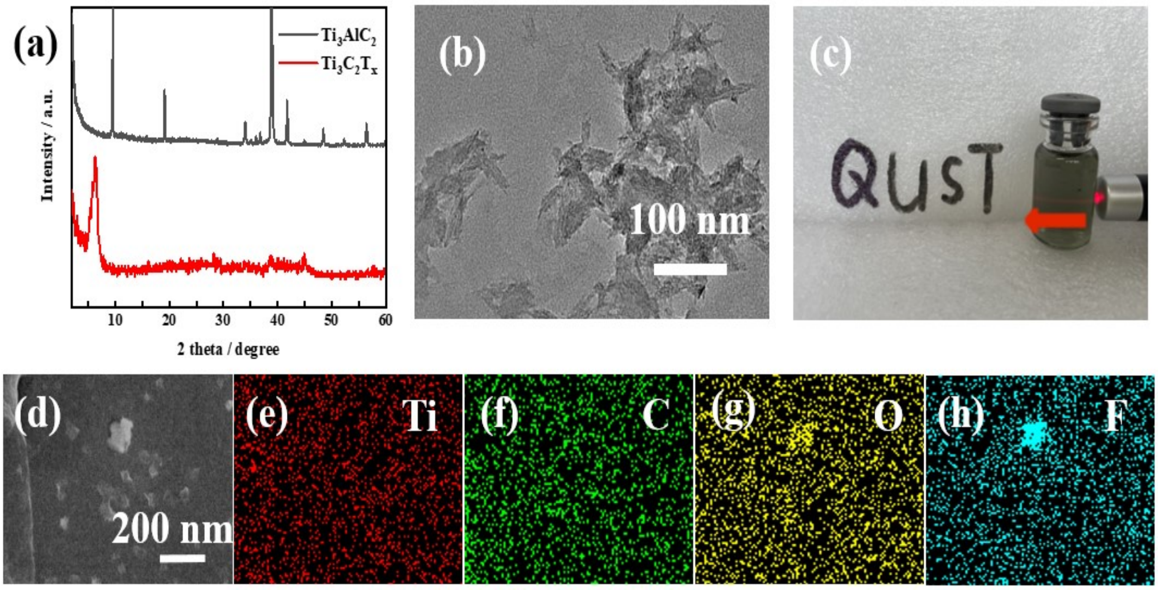

Figure S2. (a) XRD patterns of Ti_3AlC_2 MAX and $Ti_3C_2T_X$ MXenes; (b) TEM image of $Ti_3C_2T_X$ MXene; (c) Optical photograph of Tyndall phenomenon; (d)-(h) Elemental mapping images of Ti, C, O and F in Ti_3C_2 MXene.

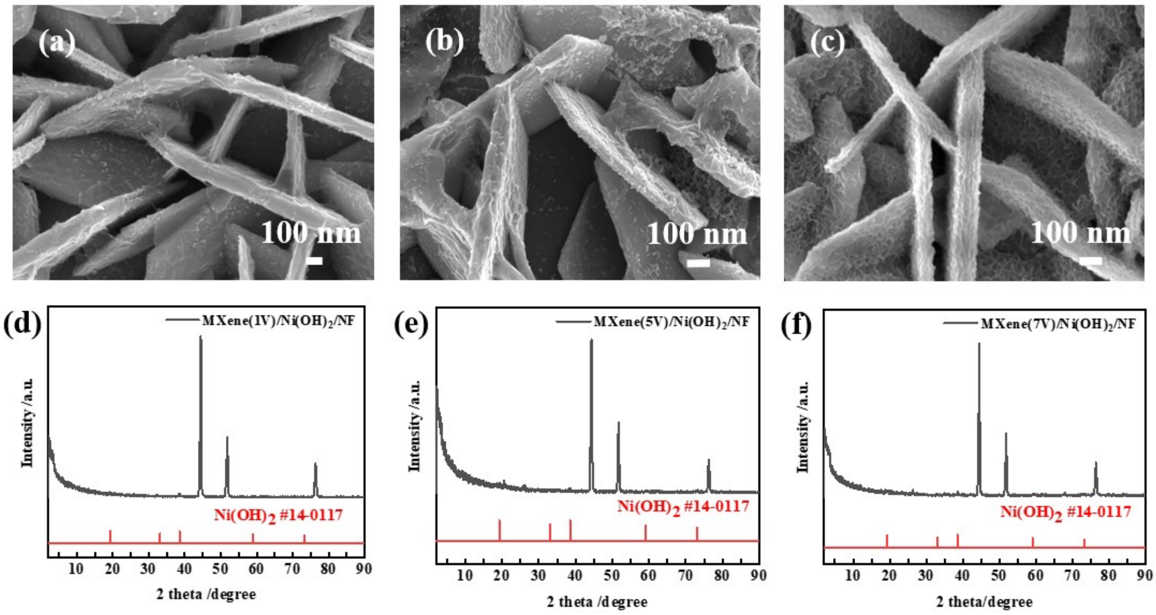

Figure S3. SEM images of (a) MXene(1 V) /$Ni(OH)_2$/NF, (b) MXene(5 V) /$Ni(OH)_2$/NF and (c) MXene(7 V) /$Ni(OH)_2$/NF; XRD images of (d) MXene(1 V)/$Ni(OH)_2$/NF, (e) MXene(5 V)/$Ni(OH)_2$/NF and (f) MXene(7 V)/$Ni(OH)_2$/NF.

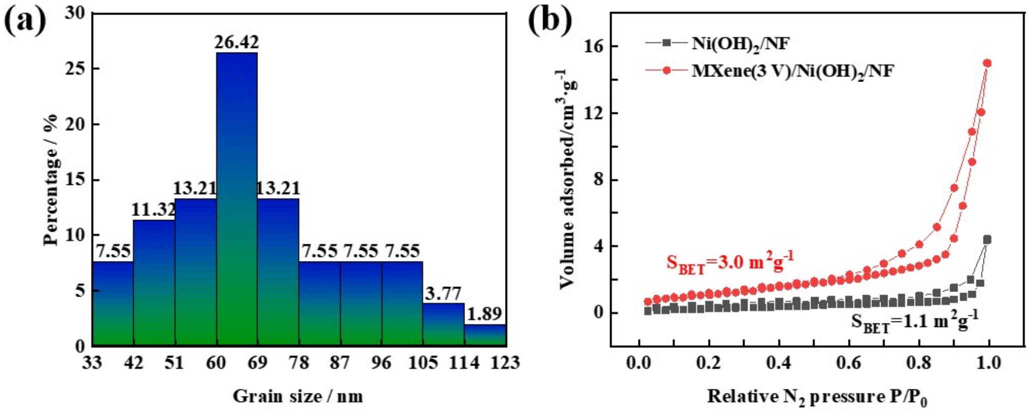

Figure S4. (a) Grain sizes of MXene in MXene/$Ni(OH)_2$/NF; (b) N_2 adsorption-desorption isotherms of $Ni(OH)_2$/NF and MXene/$Ni(OH)_2$/NF.

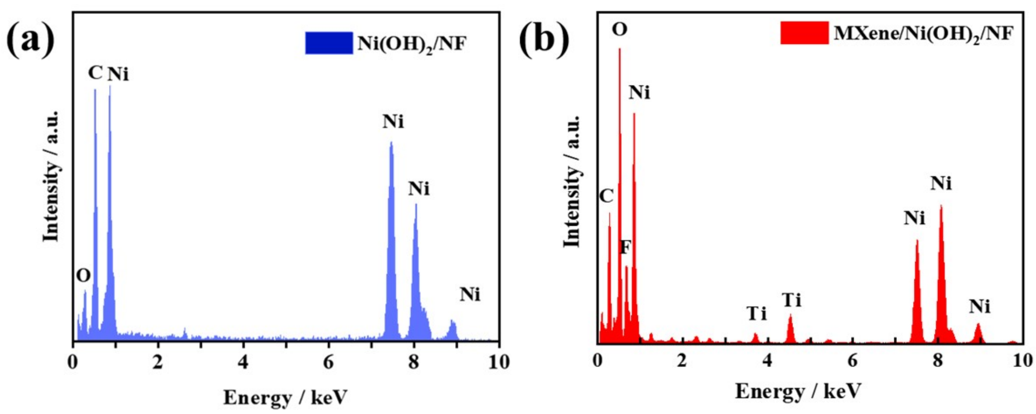

Figure S5. (a,b) EDS images of $Ni(OH)_2$/NF and $Ti_3C_2T_x$ MXene/$Ni(OH)_2$/NF.

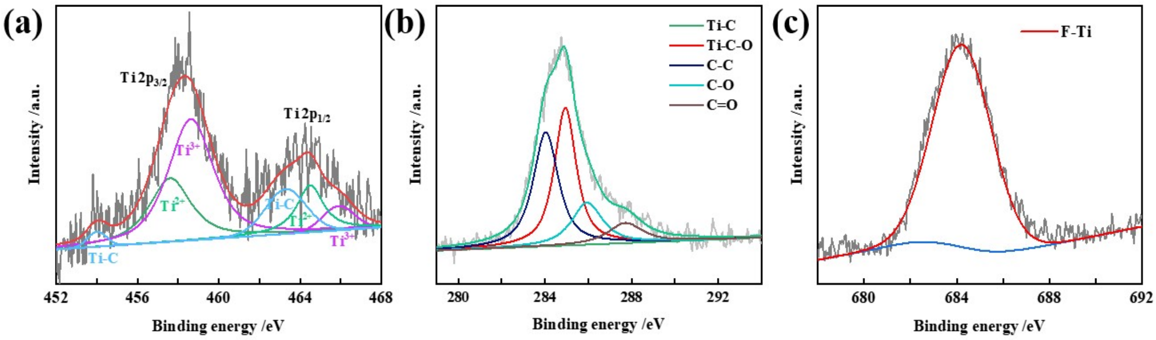

Figure S6. XPS of $Ti_3C_2T_x$ MXene/$Ni(OH)_2$/NF: (a) Ti 2p, (b) C 1s, (c) F 1s.

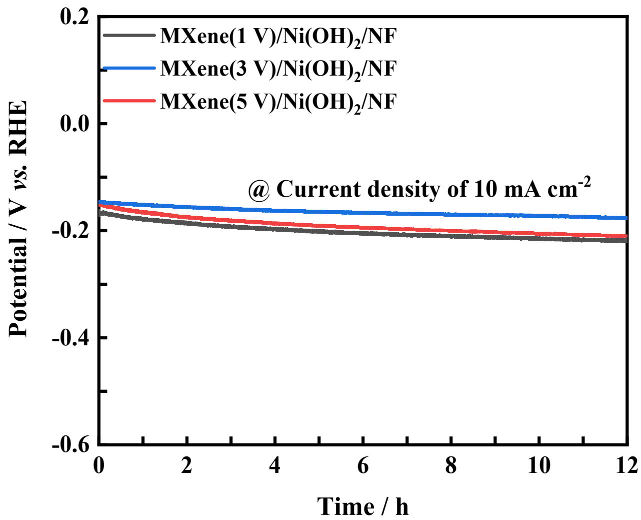

Figure S7. Chronopotential (CP) curve of the Mxene(1 V)/$Ni(OH)_2$/NF, Mxene(3 V)/$Ni(OH)_2$/NF and Mxene(5 V)/$Ni(OH)_2$/NF samples at 10 mA cm^{-2}.

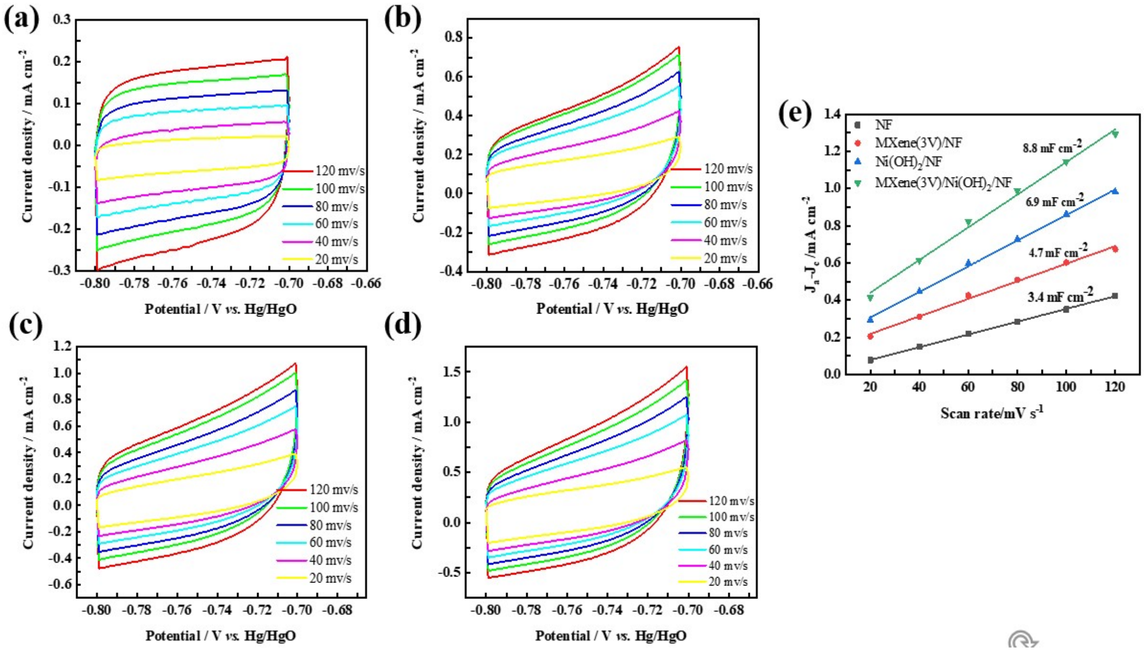

Figure S8. Cyclic voltammetry curves of (a) NF, (b) MXene(3 V)/NF, (c) $Ni(OH)_2$/NF and (d) MXene(3 V)/$Ni(OH)_2$/NF; (e) linear fitting of HER △j vs. scan rates at +0.216 V vs. RHE.

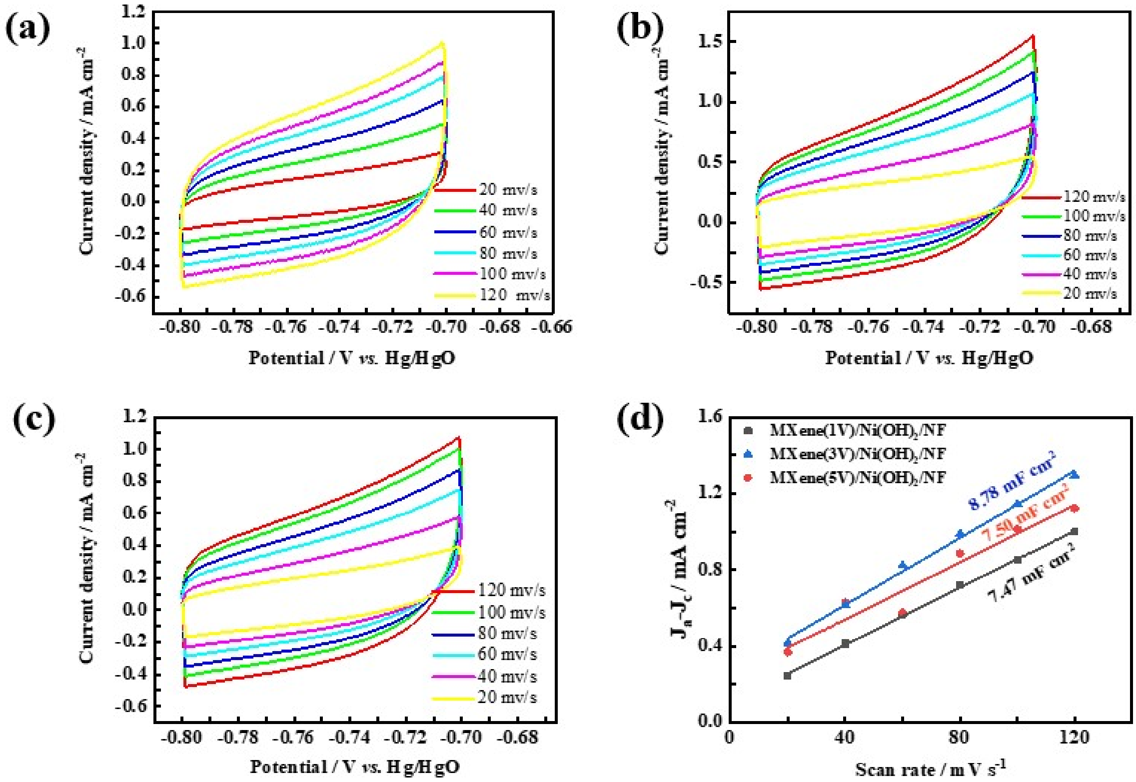

Figure S9. Cyclic voltammetry curves of (a) MXene(1V)/$Ni(OH)_2$/NF, (b) MXene(3 V)/$Ni(OH)_2$/NF, (c) MXene(5 V)/$Ni(OH)_2$/NF; (d) linear fitting of HER △j vs. scan rates at +0.216 V vs. RHE.

Table S1. HER performance of MXene/$Ni(OH)_2$/NF compared with previously reported electrocatalysts.

Catalysts	**η_{10}(mV)**	**Substrate**	**References**
$Ti_3C_2T_x$ MXene/$Ni(OH)_2$/NF	66	NF	This work
P-CoFe-LDH@MXene/NF	85	NF	Applied Catalysis B:Environmental 299 (2021) 120660
FeNi@Mo2TiC2Tx@NF	165	NF	Nano Research 2021, 14(10):3474–3481
Ni0.7Fe0.3PS3@MXene	196	--	Adv. Energy Mater. 2018, 1801127
Ni2P/NF	116	NF	NanoResearch volume 13, pages2098–2105 (2020)
Ru-NiFeP/NF	105	NF	Appl. Surf. Sci. 2021, 536, 147952
NiFeLa-LDH/v-MXene/NF	38	NF	Journal of Energy Chemistry 70 (2022) 472–479
NiO@Ni2P/NF	79	NF	International Journal of Hydrogen Energy 47 (2022) 17097-17106
NiFeS@Ti3C2 MXene/NF	180	NF	Applied Catalysis B:Environmental 321 (2023) 122039
TiVCTx@NF	151	NF	RSC Adv, 2022, 12, 23584–23594